Intestinal Adherence of *Vibrio cholerae* Involves a Coordinated Interaction between Colonization Factor GbpA and Mucin[∇][†]

Rudra Bhowmick,[1] Abhisek Ghosal,[1] Bhabatosh Das,[2] Hemanta Koley,[1] Dhira Rani Saha,[1] Sandipan Ganguly,[1] Ranjan K. Nandy,[1] Rupak K. Bhadra,[2] and Nabendu Sekhar Chatterjee[1]*

National Institute of Cholera and Enteric Diseases, Kolkata, India,[1] and Infectious Diseases and Immunology Division, Indian Institute of Chemical Biology, Kolkata, India[2]

The chitin-binding protein GbpA of *Vibrio cholerae* has been recently described as a common adherence factor for chitin and intestinal surface. Using an isogenic in-frame *gbpA* deletion mutant, we first show that *V. cholerae* O1 El Tor interacts with mouse intestinal mucus quickly, using GbpA in a specific manner. The *gbpA* mutant strain showed a significant decrease in intestinal adherence, leading to less colonization and fluid accumulation in a mouse in vivo model. Purified recombinant GbpA (rGbpA) specifically bound to *N*-acetyl-D-glucosamine residues of intestinal mucin in a dose-dependent, saturable manner with a dissociation constant of 11.2 μM. Histopathology results from infected mouse intestine indicated that GbpA binding resulted in a time-dependent increase in mucus secretion. We found that rGbpA increased the production of intestinal secretory mucins (MUC2, MUC3, and MUC5AC) in HT-29 cells through upregulation of corresponding genes. The upregulation of *MUC2* and *MUC5AC* genes was dependent on NF-κB nuclear translocation. Interestingly, mucin could also increase GbpA expression in *V. cholerae* in a dose-dependent manner. Thus, we propose that there is a coordinated interaction between GbpA and mucin to upregulate each other in a cooperative manner, leading to increased levels of expression of both of these interactive factors and ultimately allowing successful intestinal colonization and pathogenesis by *V. cholerae*.

Vibrio cholerae is the causative agent of the potentially lethal disease cholera. *V. cholerae* strains belonging to serogroups O1 and O139 are mainly responsible for cholera epidemics, while strains of other serogroups may cause sporadic outbreaks of the disease. Although the O139 strain has evolved recently, *V. cholerae* O1 biotype El Tor strains have still been responsible for most of the epidemics in recent years (20, 26). In order to cause the disease, *V. cholerae* must adhere to the intestinal mucus barrier (52). The ability of *V. cholerae* to adhere to animal cells has been studied before (26, 42), and various adherence factors have been proposed, including the virulence-associated toxin-coregulated pilus (5), outer membrane proteins (26, 42), and lipopolysaccharide (LPS) (11). Attachment of *V. cholerae* to abiotic surfaces has also been recently described (50). However, there is still no information about the factor(s) responsible for initial adherence of the bacteria to the intestine and whether the host plays any role in aiding the colonization of the intestine by the bacteria.

Vibrios are marine organisms that adhere to chitin in the environment (12, 33) and utilize chitin as the sole source of nitrogen and carbon by using a family of glycosyl hydrolases, called chitinases (21). Genome analysis of *V. cholerae* O1 El Tor has revealed the presence of seven such chitinase genes (7), some of which have been characterized (27, 37). One of

these genes is the putative chitinase gene with locus number VCA0811, the product of which has been recently identified as a common adhesion molecule for both chitinous and intestinal surfaces for a *V. cholerae* O1 classical isolate (29). This gene product has been designated *N*-acetyl-D-glucosamine (GlcNAc)-binding protein A (GbpA). Interestingly, this gene remains constitutively expressed under different growth conditions in *V. cholerae* compared to other species of vibrios (7).

The epithelial surface of the mammalian intestine is covered by a mucus layer, which prevents most microorganisms from reaching and persisting on the intestinal surface (16). This viscoelastic gel (3) is protective against adhesion and invasion by many pathogenic microorganisms. The principal component of mucus is a complex, high-molecular-weight ($>2 \times 10^6$) glycoprotein (mucin) that is responsible for the characteristic visco-elastic properties of the secretion (41). Mucins are diverse molecules and contain large quantities of different carbohydrate-containing modifications, but the monomer of chitin, GlcNAc, forms a bulk of the sugars present in it (39). Previous studies have shown that the glycoproteins of mucus can act as receptors for vibrios (2), but the adhesin responsible for this attachment of *V. cholerae* has not yet been identified.

In this study, using purified recombinant GbpA (rGbpA) and an isogenic in-frame *gbpA* deletion mutant, we show that GbpA binds to mucin, the first surface to which *V. cholerae* is exposed in the intestine (52) for colonization and pathogenesis of *V. cholerae* in a mouse model. We also show that the initial intestinal adherence of *V. cholerae* increases mucin secretion in the intestine, which again increases the expression of GbpA in the bacteria. We thus propose that the initial adherence of *V. cholerae* to the intestine involves a coordinated interaction between GbpA and intestinal mucin.

---

* Corresponding author. Mailing address: Division of Biochemistry, National Institute of Cholera and Enteric Diseases (Indian Council of Medical Research), P-33 C.I.T. Road, Beliaghata, Kolkata 700 010, India. Phone: 91 (33) 2370-4598. Fax: 91 (33) 2370-5066. E-mail: chatterjeens@icmr.org.in.

MATERIALS AND METHODS

Bacterial strains and cell culture. *V. cholerae* O1 biotype El Tor strain N16961 was used as the wild-type strain in this study. Bacteria were grown at 37°C in Luria-Bertini (LB) broth or on LB agar. Appropriate antibiotics were used at the required concentrations (streptomycin at a final concentration of 100 μg/ml, ampicillin at 50 or 100 μg/ml, and kanamycin at 45 μg/ml). The green fluorescent protein (GFP) plasmid pG13 and the suicide vector pKAS32 were made available to us by Karl E. Klose of the University of Texas, San Antonio. The human colon cancer cell line HT-29 (National Center for Cell Sciences, Pune, India) was grown to confluence in six-well plates according to a previously described protocol (9). Cells were serum starved overnight prior to experiments.

Construction of a *V. cholerae* Δ*gbpA* strain and its complementation with plasmid pGbpAS. Construction of Δ*gbpA V. cholerae* was done by a procedure as described before (46). Briefly, two fragments from the two ends of *gbpA* of *V. cholerae* N16961 were PCR amplified using the primer pairs EXT1F (5′-GGCT ACGTTTCCGCAGT-3′; nucleotides [nt] 73 to 89) with FUS1R (5′-<u>GTCGTA GTCACCCGG</u>**CTGGTTTGGGGTTCCAGTTTG**-3′; nt 1275 to 1261 are underlined and nt 417 to 398 are in bold) and FUS1F (5′-**TGGAACCCAAACCAG**<u>CC GGGTGACTACGACTTTG</u>-3′; nt 403 to 420 are in bold and nt 1261 to 1279 are underlined) with EXT1R (5′-ACGTTTATCCCACGCCATT-3′; nt 1455 to 1437), to generate 345-bp and 195-bp amplicons, respectively. The amplicons were fused and amplified with the primer pair EXT1F and EXT1R, to generate a 540-bp amplicon with an in-frame deletion of 845 bp (nt 418 to 1260) of *gbpA*. The amplicon was subcloned into the suicide vector pKAS32 (46). The resultant plasmid, pKAG, was transformed into *Escherichia coli* SM10λ*pir* (38) and maintained in the same strain. To generate an insertion mutant within the *gbpA* gene of N16961, plasmid pKAG was mobilized conjugally from SM10λ*pir* into N16961, and the transconjugants (designated N1RB2) were selected on minimal agar plates containing 20% glucose and 50 μg/ml ampicillin. The transconjugants with an insertion of pKAG in the *gbpA* locus were further passaged on LB agar plates with 100 μg/ml streptomycin for the removal of the pKAG vector backbone and to achieve an in-frame deletion of *gbpA*. The isogenic in-frame *gbpA* deletion mutants thus generated were termed N1RB3. In-frame deletion of *gbpA* was confirmed by PCR assay followed by nucleotide sequence analysis. The deactivation of GbpA due to in-frame deletion was checked through a chitin-binding assay, as described before (40). N1RB3 was complemented with plasmid pGbpAS to generate strain N1RC2, following a previously described procedure (29). The replacement of GbpA was confirmed by Western blotting and binding assay as described above.

Studies of bacterial binding to intestine. The *V. cholerae* strains (N16961, N1RB3, and N1RC2) were electroporated with pG13 and maintained on LB agar plates additionally supplemented with kanamycin. Intestinal segments were isolated from BALB/c mice, washed, and fixed (51). The washed mucosal sides were used immediately for adhesion experiments. Pieces of mucosa were immersed in GFP-labeled bacterial suspension (1×10^7 CFU/ml in Krebs-Ringer-Tris [KRT] buffer, pH 7.4) and incubated for 30 min at 28°C. The sections were washed several times in KRT buffer (pH 7.4), mounted on glass slides, and observed under a confocal microscope (Zeiss LSM 510 META) at a magnification of ×40 (excitation, 470 nm; emission, 510 nm).

The number of adherent *V. cholerae* cells was calculated from the fluorescence intensities of confocal images, using LSM 510 software (Carl Zeiss, Germany), by a previously described method (49). For this, eight randomly selected images were collected from each tissue piece, and each image was processed as 10 *z* sections. After background subtraction, fluorescence intensities of whole images were measured. The fluorescence intensities of 8 to 10 single bacterial cells from each image were also measured, and the average intensity of a single bacterium was calculated. The number of adherent *V. cholerae* cells was then calculated as follows: number of bacteria = (fluorescence intensity of whole image)/(fluorescence intensity of single bacterium).

Intestinal colonization and fluid accumulation assays. Animal experiments were conducted following the guidelines of the Institutional Animal Ethical Committee. Infection and recovery of *V. cholerae* from infant mouse intestine were done as previously described (47). Briefly, 4- to 5-day-old BALB/c mice were separated from their mothers 2 hours prior to oral inoculation with 100 μl of diluted cultures of *V. cholerae* N16961, N1RB3, or N1RC2. Infected mice were kept in the absence of their mothers. Mice were sacrificed, and their entire intestines removed and mechanically homogenized in 2 ml LB containing 20% (vol/vol) glycerol. Serial dilutions were plated onto LB agar with appropriate antibiotics to enumerate *V. cholerae* CFU per segment (4). Undiluted samples were plated as controls.

Fluid accumulation was assayed as described previously (6). Infected mice were sacrificed after 4, 8, 12, or 18 h and weighed, and their entire intestines were

removed. Each of the separated intestines was weighed. The fluid accumulation ratio was calculated as intestinal weight/(whole body weight − intestinal weight) (6). Mice fed phosphate-buffered saline (PBS) were used as negative controls.

Intestinal mucus secretion assay. The intestinal mucus secretion assay was performed by a previously described method (15), with modifications. Briefly, adult BALB/c mice were kept without food for 24 h and orally incubated with 1 ml of overnight cultures of *V. cholerae* N16961, N1RB3, or N1RC2. Small intestines were collected, washed several times, and put into binding buffer (3.84 mM NaH$_2$PO$_4$, 6.16 mM Na$_2$HPO$_4$, 0.15 M NaCl, pH 7.2). Intestines were split along the mesenteric border, and mucus was collected by gentle scraping. All processes were performed in an ice bath. The scrapings were pooled, centrifuged (10,000 × *g*, 4°C, 15 min), and the supernatant containing crude mucus was collected. Concentrations of protein and neutral and acidic sugars were measured by previously described methods (14, 34, 35). The mucus concentration was also measured by blotting the mucus on polyvinylidene difluoride membranes and staining it with periodic acid-Schiff reagent (PAS) or pH 2.5 Alcian blue (AB) (1).

Histopathology. Intestines of orally inoculated adult BALB/c mice were processed for histopathological studies. After washing with cold PBS (pH 7.4), 5-cm pieces of ileal sections were fixed in 10% formalin-KRT buffer and processed for paraffin embedding. Serial 5-μm-thick sections were cut, placed on glass slides, and stained with hematoxylin and eosin. All samples were examined by light microscopy (Leica DMLB), and digital photographs (magnification, ×20) of the stained tissues were taken. For measurement of the thickness of mucus layers, five randomly selected sections were analyzed, using Leica QWin software. Three animals were used for each experiment.

Cloning, expression, and purification of rGbpA and raising of antiserum. The *gbpA* gene (without its amino-terminal signal sequence and with the stop codon) was PCR amplified using a genomic DNA preparation of *V. cholerae* N16961 with the primer pair G1F (5′-GGCTACGTTTCCGCAGT-3′) and G1R (5′-TT AACGTTTATCCCACG-3′). The amplicon was cloned into the pBAD-TOPO cloning-expression vector (Invitrogen, Carlsbad, CA), and the resultant plasmid was designated pGbpA. *gbpA*, including its amino-terminal signal sequence, was also PCR amplified similarly using the primer pair G2F (5′-ATGAAAAAACA ACCTAAAATG-3′) and G1R (5′-TTAACGTTTATCCCACG-3′). The amplicon was cloned into the above-mentioned vector, and the construct was designated pGbpAS. All the plasmids were amplified in *E. coli* TOP10 cells and confirmed by DNA sequencing.

To generate the rGbpA, the *E. coli* transformants were induced with 0.02% arabinose overnight at 30°C. The induced bacteria were harvested, washed, resuspended in buffer (20 mM Tris-Cl [pH 7.4] with 1 mM dithiothreitol, 5 mM phenylmethylsulfonyl fluoride, and 10% glycerol), and sonicated. Unbroken cells were removed by centrifugation. Purification of rGbpA from the supernatants was done by a previously described method (17). Twenty-milliliter aliquots of cell-free lysates were incubated with 100 mg colloidal chitin. After agitation of the suspension for 60 min at room temperature, the colloidal chitin was collected by centrifugation and extensively washed with 20 mM Tris-HCl (pH 7.4). Finally, rGbpA was eluted with 0.05 M HCl and neutralized by addition of 0.1 M Tris-HCl, pH 8.0. The activity of the released rGbpA was checked by its ability to rebind chitin. The rGbpA was devoid of any LPS contamination as examined by neutral sugar estimation (14). The protein was also subjected to sodium dodecyl sulfate-polyacrylamide gel electrophoresis (SDS-PAGE) with or without protease treatment, and silver staining of the gel confirmed the absence of LPS (data not shown).

BALB/c mice were injected intraperitoneally with purified rGbpA to raise the polyclonal antibody according to standard procedures.

Purification of mucus, mucin, and IEC and their brush borders. BALB/c mouse intestine was used for all purification processes. Mucus was first purified from mouse intestine; mucin was then prepared from it by isopyknic ultracentrifugation in cesium chloride (36). Primary intestinal epithelial cells (IEC) and their brush borders were isolated by previously described methods (13, 19). IEC were used at a concentration of 2×10^6 cells/ml and were stimulated for different time points in 5% CO$_2$ at 37°C with rGbpA.

Binding of rGbpA with different substrates. To quantitate the binding of rGbpA to mucus, mucin, IEC, and brush borders, an enzyme-linked immunosorbent assay (ELISA) was performed according to a modification of a previous protocol (43). The substrates were precoated overnight in triplicate in 96-well microtiter plates at 4°C. After washing, rGbpA was added to the wells at different concentrations (0 to 1 μg/μl) and incubated at 25°C for 1 h. ELISA was performed using anti-rGbpA antibody (1:100) and horseradish peroxidase-conjugated secondary antibody (1:1,000). Color developed using 3,3′,5,5′-tetramethylbenzidine (BD Biosciences, Palo Alto, CA) was measured at 450 nm, and binding was quantitated. For study of sugar specificity, different concentrations
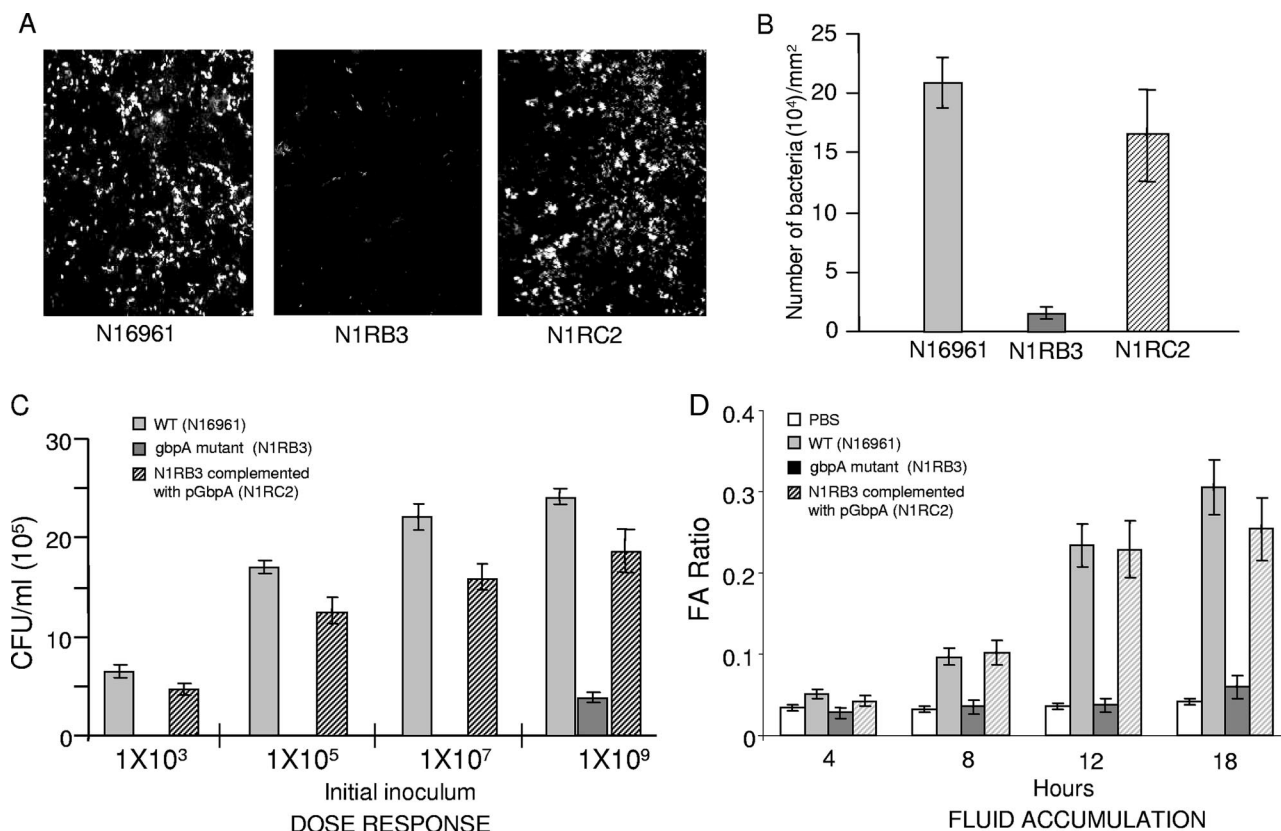
FIG. 1. Effect of *gbpA* mutation of *V. cholerae* on intestinal colonization. GFP-labeled *V. cholerae* strains (N16961, N1RB3, and N1RC2) were allowed to bind to mouse ileal segments for 30 min. Sections were washed several times in buffer, mounted on glass slides, and observed under a confocal microscope at a magnification of ×40. (A) Confocal images of representative intestinal sections, showing adherent, fluorescent *V. cholerae*. (B) Number of adherent bacterial cells calculated from fluorescence intensities. The number of bacteria calculated from eight independent intestinal sections is presented graphically. (C) Four- to 5-day-old BALB/c mice were intragastrically inoculated with increasing initial bacterial inoculum (1×10^3 to 1×10^9 CFU) of *V. cholerae* strains (N16961, N1RB3, or N1RC2) as indicated. Mice were sacrificed after 18 h; intestinal segments were aseptically removed and processed for bacterial quantification. Bars show recovery from mouse intestines with respect to initial bacterial inoculum. Data represents means ± SEM from six independent experiments. (D) Fluid accumulation in mouse intestines challenged with *V. cholerae* strains (N16961, N1RB3, or N1RC2). Four to 5-day-old BALB/c mice were intragastrically inoculated with bacterial inoculum of 1×10^5 CFU of *V. cholerae* strains (N16961, N1RB3, or N1RC2) as indicated. Mice were sacrificed after 4, 8, 12, and 18 h. The fluid accumulation ratio was calculated and presented graphically. PBS was used as negative control. Data represent means ± SEM of six independent experiments. WT, wild type.

of rGbpA were preincubated with 2% GlcNAc (Sigma, St. Louis, MO) at room temperature for 30 min before being added to the wells.

Curve fitting. The rGbpA bound to purified intestinal mucin, mouse IEC, and brush border membrane was calculated from the absorbance reading, and the maximum binding was assigned the value 1. Data fitting was done using Kyplot version 2.0 Beta15 (32 bit) to obtain the best-fit curves to obtain the dissociation constant (K_d). Values are the means of triplicate determinations from two separate experiments.

Analysis of mucin levels in HT-29 cells. HT-29 cells were treated with purified rGbpA (100 ng/well). After 30 min to 4 h of incubation at 37°C in 5% CO_2, the culture medium was aspirated at different time points and kept at 4°C until use. Secretory mucin levels were analyzed by ELISA as described before, using antibodies against MUC2, MUC3, and MUC5AC (Santa Cruz Biotechnology, Santa Cruz, CA). Absorbance was measured at 492 nm. Similarly, the cells were treated with 0 to 200 ng/well of rGbpA for 1 h; levels of secretory mucins were analyzed by ELISA as described above. Bovine serum albumin was used as a negative control.

The increase in transcripts of the *MUC2*, *MUC3*, and *MUC5AC* genes under the conditions described above was determined by reverse transcription-PCR (RT-PCR). Total RNA was isolated from rGbpA-treated or untreated HT-29 cells by the standard Trizol (Invitrogen) method. Transcript levels were analyzed by RT-PCR using specific primers (18). β-Actin was used as an internal control. For each of the mucin transcripts and β-actin, the linear range of PCR ampli-

fication was verified by quantifying the RT-PCR product obtained after amplifications for 15 to 35 cycles (data not shown). All PCRs were performed for 25 cycles, which was within the linear range of amplification of the corresponding mRNA species. The products were run on 1% agarose gels, stained with ethidium bromide, and finally quantitated using Quantity One software (Bio-Rad). All of the amplified RT-PCR products were normalized with respect to the β-actin RT-PCR product.

Nuclear extracts and assessment of NF-κB translocation. Nuclear extracts were prepared from rGbpA-treated HT-29 cells (45) at different incubation times (0 to 45 min) and rGbpA concentrations (0 to 200 ng/well). Untreated cells were used as negative controls. The nuclear content of NF-κB was determined by Western blot analysis using NF-κB p65 antibody (BD Biosciences) as described above. IκBα levels in the cytosol were similarly determined with anti-IκBα antibody (Cell Signaling, Beverly, MA) (25). To block nuclear translocation of NF-κB, HT-29 cells were pretreated with the proteasomal inhibitor MG132 (Calbiochem, La Jolla, CA) (20 μM final concentration) for 30 min, prior to rGbpA treatment (24).

Analysis of GbpA levels in *V. cholerae*. N16961 and N1RB3 were grown in the presence of 0 to 4% mouse intestinal mucin overnight. RT-PCR was performed with 5 μg of total RNA and analyzed using a gel documentation system (Bio-Rad) as described before (7). The *recA* gene (VC0015, accession no. AE004093) was used as an internal control.

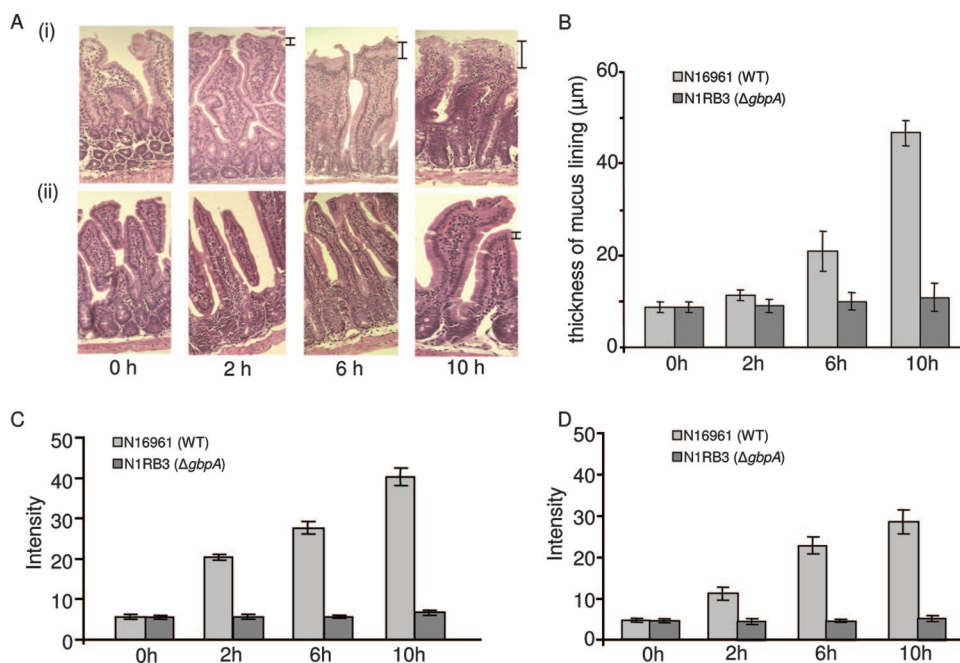Bacterial membrane and culture supernatant were isolated (44), and GbpA

FIG. 2. Effect of *V. cholerae* binding to intestine. Adult BALB/c mice were intragastrically inoculated with 1×10^7 CFU/ml of *V. cholerae* strains (N16961, N1RB3, or N1RC2). After incubation for 0, 2, 6, or 10 h, the intestines were processed for histopathological studies. Five-micrometer-thick sections from paraffin-embedded intestinal segments were cut, placed on glass slides, and stained with hematoxylin and eosin. All samples were examined by light microscopy, and digital photographs were taken at a magnification of ×20. (A) Histopathology of mouse intestinal sections, showing mucus secretion at different time points. (i) Intestine challenged with N16961; (ii) intestine challenged with N1RB3. The thickness of mucus layers was analyzed. The increase in mucus thickness is marked on the side. Images presented are representative of results obtained in three separate experiments. (B) Time-dependent increase of the thickness of mucus lining on the intestine. Data represent means ± SEM from three independent experiments. WT, wild type. (C and D) Parts of the intestines were used to isolate mucus. The isolated mucus was blotted on polyvinylidene difluoride membranes; the membranes were stained either with PAS(C) or pH 2.5 AB (D). The dots were analyzed densitometrically, quantitated, and plotted graphically. The bar diagram shows dot blot intensities after staining. Data represents mean ± SEM from three independent experiments.

levels were analyzed by standard Western blotting using anti-rGbpA polyclonal antibody. Membrane-bound GbpA on strain N16961 grown in the absence or presence of mucin was analyzed by confocal microscopy. Bacteria were incubated with anti-rGbpA antibody followed by fluorescein isothiocyanate-conjugated secondary antibody. Bacteria were then visualized under a confocal microscope.

Statistical analysis. Wherever applicable, the results represented in this paper are means ± standard errors of the mean (SEM) from at least three separate experiments. Statistical differences were analyzed by analysis of variance with the level of significance being set at 5% ($P < 0.05$).

Nucleotide sequence accession number. The sequence of the *gbpA* open reading frame has been deposited in GenBank with accession number EU072441.

RESULTS

Generation of a *V. cholerae* in-frame *gbpA* deletion mutant strain. To test the hypothesis that GbpA is needed for initial intestinal adhesion by *V. cholerae*, an isogenic in-frame deletion mutant of *gbpA* was generated from N16961. The isogenic in-frame deletion mutant N1RB3 did not produce GbpA and failed to bind chitin flakes (see Fig. S1 in the supplemental material). Both wild-type and mutant strains grew on thiosulfate-citrate-bile salt-sucrose (TCBS) agar, were oxidase positive, and were positive for cholera toxin. When N1RB3 was complemented with the intact *gbpA* gene through the plasmid pGbpAS (N1RC2), the production of GbpA was restored with concomitant restoration of the chitin-binding phenotype (see Fig. S1 in the supplemental material).

Adherence of *V. cholerae* to the intestinal mucosa. Adherence of N16961, N1RB3, and N1RC2 strains to the mucus surface of the mouse intestine was observed within 30 min by confocal microscopy (Fig. 1A). When quantitated, the number of N1RB3 bacteria adhering to the intestinal section was 11.4-fold less than the number of adherent N16961 bacteria ($P < 0.05$) (Fig. 1B). For N1RC2, the number of adherent bacteria was ninefold more that of the N1RB3 strain ($P < 0.05$) (Fig. 1B).

Role of GbpA in *V. cholerae* pathogenesis. Pathogenesis was studied based on two parameters: dose response and fluid accumulation in infant mice. The number of bacteria recovered from the intestine increased with the increase in initial bacterial inoculum for N16961. N1RB3 gave colonies on LB agar plates only at the highest initial inoculum, but its recovery was 6.3-fold less than that of N16961 at the same inoculum ($P < 0.01$). N1RC2 showed significant reversal of the phenotype, and the number of N1RC2 bacteria recovered from the intestine was 4.8-fold more than that of N1RB3 ($P < 0.01$) at the highest initial inoculum (Fig. 1C).

When fluid accumulation with respect to time was calculated, mice infected with N16961 showed an increase in fluid accumulation at 4 h, whereas mice incubated with N1RB3 did not show any increase in the first 12 h ($P = 0.442$). Fluid accumulation by N1RB3 was 5.1-fold less than that by N16961
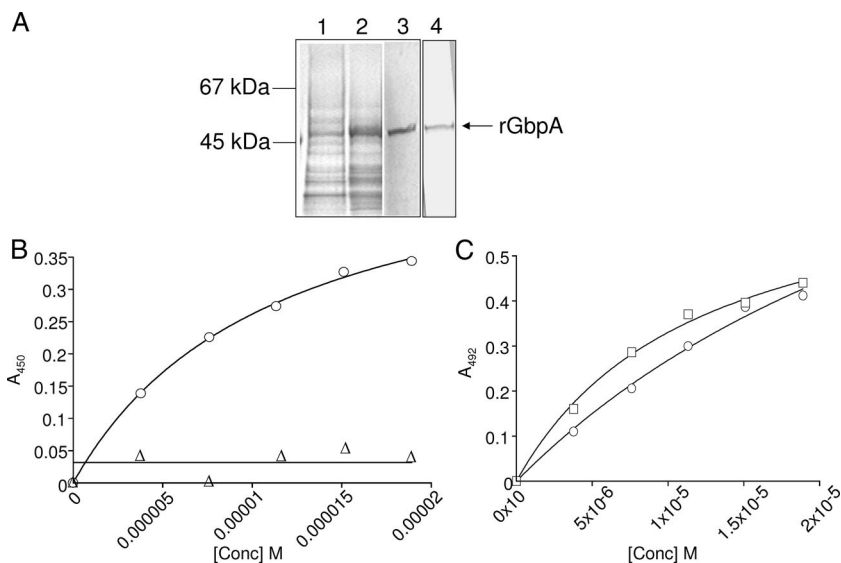
FIG. 3. Expression and purification of rGbpA and its interaction with mucin, mouse IEC, and their brush borders. (A) Expression and purification of rGbpA. Lanes 1 to 3, proteins were analyzed by 10% SDS-PAGE and visualized by Coomassie blue staining. Lane 1, total cell lysate of uninduced TOP10-*gbpA* (10 µg); lane 2, total cell lysate of TOP10-*gbpA* induced with 0.02% arabinose (10 µg); lane 3, purified rGbpA (10 µg). Lane 4, immunoblot of purified rGbpA with anti-rGbpA polyclonal antibody. (B) Graphical representation of binding of rGbpA to purified mucin and the inhibition by GlcNAc as determined by ELISA. Various concentrations of rGbpA (○) were allowed to bind to 0.1 µg immobilized mucin for 1 h. The best-fit curve showed the K_d with 0.1 µg mucin to be 11.2 µM. Preincubation with 2% GlcNAc inhibited the binding of rGbpA (△)-immobilized mucin (0.1 µg). Values are the means of triplicate determinations from two separate experiments. (C) Graphical representation of binding of rGbpA to mouse IEC and their brush borders as determined by ELISA. Various concentrations of rGbpA were allowed to bind to mouse IEC (□) and their brush borders (○) for 1 h. The best-fit curve showed the K_d to be 17.2 and 12 µM for mouse IEC and their brush borders, respectively. Values are the means of triplicate determinations from two separate experiments.

at 18 h of incubation ($P < 0.01$), while the fluid accumulation by N1RC2 was 4.2-fold more than that by N1RB3 at the same time point ($P < 0.01$). PBS-fed mice showed no significant variation in fluid accumulation over the experimental time points ($P = 0.169$) (Fig. 1D). The results thus suggest that GbpA is a key factor for pathogenesis.

GbpA-mediated binding of *V. cholerae* increases mucus secretion. The increase in the intestinal mucus secretion due to the GbpA-mediated binding of *V. cholerae* was determined by histopathology (Fig. 2A). The thickness of the mucus layer increased in a time-dependent manner in case of N16961, beginning within 2 hours of bacterial binding, and was 2.4-fold at 6 h ($P < 0.05$), and 5.3-fold at 10 h with respect to the mucus layer thickness at 0 h ($P < 0.01$) (Fig. 2B). When challenged with N1RB3, the thickness of mucus layer remained almost unchanged ($P = 0.344$) over the experimental time period. The thickness of the mucus coat in this case was 2.1-fold less ($P < 0.05$) at 6 h and 4.3-fold less ($P < 0.01$) at 10 h than the thickness of the mucus layer of the intestines after N16961 challenge (Fig. 2B).

The increase in intestinal mucus secretion was also confirmed by blotting assays with PAS (Fig. 2C) and AB staining (Fig. 2D) of concentrated perfusates obtained from the intestines challenged either with N16961 or with N1RB3. PAS staining showed a 7.2-fold increase ($P < 0.01$) in mucus secretion in the N16961-challenged intestine at 10 h compared to mucus secretion at 0 h. The mucus of the intestine challenged with N1RB3 remained almost unchanged ($P = 0.165$) over the experimental time period (Fig. 2C). Compared to mucus secretion at 0 h, AB staining showed a 6.1-fold increase ($P <$

0.01) in mucus secretion in the N16961-challenged intestine at 10 h, while the mucus of the intestine challenged with N1RB3 remained almost unchanged ($P = 0.171$) over the experimental time period (Fig. 2D). Biochemical tests for sugar and protein also yielded similar information, where mucus secretion in intestines challenged with N16961 increased in a time-dependent manner and there was a negligible increase in mucus in the N1RB3-challenged intestines (data not shown).

Expression of rGbpA. *V. cholerae* El Tor N16961 *gbpA* (GenBank accession no. EU072441) was a 1.5-kb fragment. Amino acid sequence alignment with 12 other bacterial chitin-binding proteins (48) showed that the binding region of GbpA is highly conserved. The key amino acids essential for GlcNAc oligomer binding (Y52, E53, E58, H139, and D179) were in perfect alignment with these chitin-binding proteins (data not shown). Expression of rGbpA in *E. coli* TOP10 cells was analyzed by SDS-PAGE, showing the matured expressed protein to be approximately 51 kDa. The rGbpA was purified by chitin affinity chromatography. The polyclonal antibody generated specifically bound purified recombinant protein (Fig. 3A) as well as the native protein (see Fig. 6).

Binding of rGbpA with purified mucin, IEC, and brush border membranes. The ability of GbpA to directly bind to purified mucin, mouse IEC, and their brush border membranes was investigated with purified rGbpA. rGbpA bound to immobilized mucin (Fig. 3B) in a concentration-dependent and saturable manner with a K_d of 11.2 µM. Preincubation of rGbpA with 2% GlcNAc specifically inhibited its binding with mucin. K_ds for epithelial cells and brush border binding were 17.2 and 12 µM, respectively (Fig. 3C). Similarly, when rGbpA
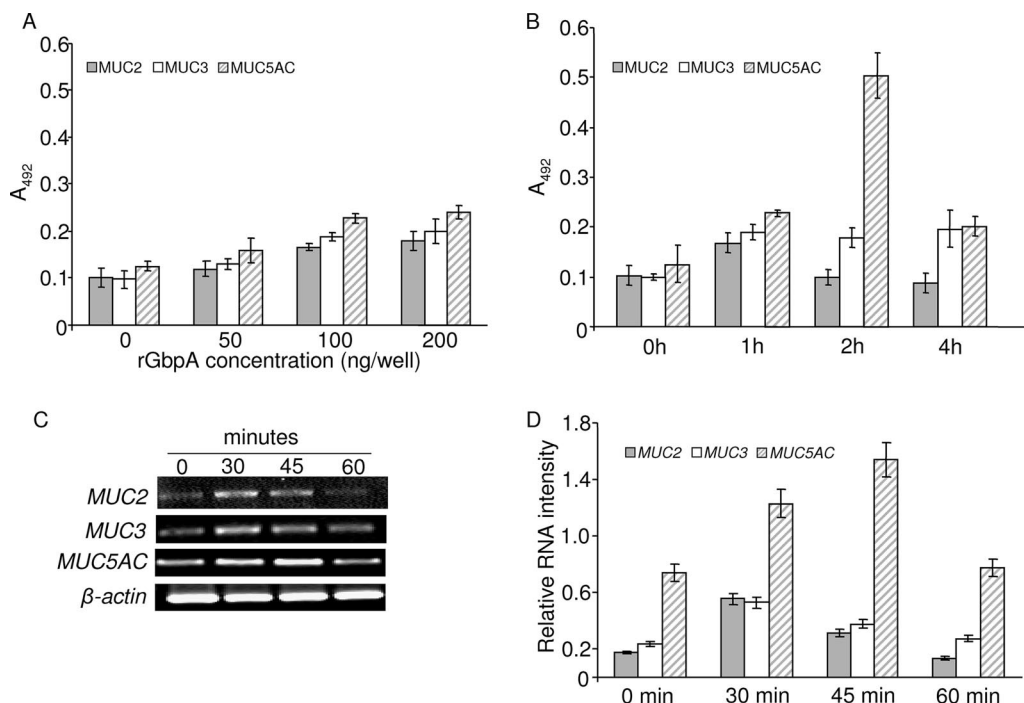
FIG. 4. Effect of rGbpA on mucin regulation. (A) rGbpA increased mucin secretion in a concentration-dependent manner. Medium was aspirated from HT-29 culture plates after 1 h of incubation with 0, 50, 100, and 200 ng/well purified rGbpA. ELISA was performed to study mucin levels using anti-MUC2, -MUC3, or -MUC5AC polyclonal antibodies. The bar diagram shows absorbance at 492 nm. Data represent means ± SEM from three independent experiments. (B) rGbpA increased mucin secretion in a time-dependent manner. Medium was aspirated from HT-29 culture plates after incubation with 100 ng/well purified rGbpA for 0, 1, 2, and 4 h, and ELISA was performed. The bar diagram shows absorbance at 492 nm. Data represent means ± SEM from three independent experiments. (C) rGbpA induced mucin gene expression. Total RNA was isolated from HT-29 cells after incubation with 100 ng/well purified rGbpA for 0, 30, 45, and 60 min. RT-PCR was performed with primers specific for the *MUC2*, *MUC3*, *MUC5AC*, and β-actin genes. Equal amounts of RT-PCR products were run on 1% agarose gels and visualized following ethidium bromide staining. A representative gel picture from three independent experiments is shown. (D) Normalized RT-PCR results are represented graphically. Equal amounts of RT-PCR products were run on 1% agarose gel and stained with ethidium bromide. Gel images were analyzed densitometrically. The β-actin gene was taken as the internal control. PCR products were quantitated and expressed with respect to β-actin band intensity, which was taken as 1. Data represent means ± SEM from three independent experiments.

was preincubated with 2% GlcNAc, binding to these substrates were not observed (data not shown). Taken together, the results suggest that GbpA binds directly to GlcNAc residues in a specific manner.

Effect of GbpA on mucin secretion. To provide direct evidence that GbpA could increase mucus secretion, HT-29 cells were treated with rGbpA. When cells were treated with 0 to 200 ng/well rGbpA for 1 h, we observed increased secretion of all three mucins tested (MUC2, MUC3, and MUC5AC) in a concentration-dependent manner (Fig. 4A). MUC2 increased by 1.64-fold ($P < 0.05$) and MUC3 and MUC5AC almost doubled with 100 ng/well rGbpA ($P < 0.05$).

Similarly, rGbpA treatment for 0 to 4 h showed that all the three secretory mucins that were tested showed increased secretion within the first hour (Fig. 4B). MUC2 increased by 1.6-fold ($P < 0.05$), and MUC3 and MUC5AC doubled within 1 h ($P < 0.05$). MUC2 secretion returned back to control level within 2 h, whereas MUC3 maintained its increased level for at least 4 h. MUC5AC secretion was fourfold greater than that for the control ($P < 0.05$) after 2 h but returned to the control level by 4 h. Bovine serum albumin treatment of HT-29 cells did not stimulate mucus secretion (data not shown).

The relative mRNA expression of *MUC2*, *MUC3*, and *MUC5AC* following incubation with rGbpA was studied by

RT-PCR at earlier time points between 0 and 60 min (Fig. 4C and D). Expression of *MUC2*, *MUC3*, and *MUC5AC* increased 3-fold, 2-fold, and 1.6-fold, respectively ($P < 0.05$), within 30 min. *MUC5AC* expression was twofold compared to the control ($P < 0.05$) after 45 min but returned back to the normal level by 1 h. Expression of the other two genes started to return back after 30 min of rGbpA treatment. The increased levels of *MUC2*, *MUC3*, and *MUC5AC* mRNAs suggested that the increased secretion of mucins under the influence of rGbpA might be regulated at the transcriptional level.

Involvement of NF-κB in mucin secretion by rGbpA. Since NF-κB is a key downstream effector during bacterial infection, we further investigated the involvement of NF-κB in mucin transcript upregulation. First, a time- and concentration-dependent effect of rGbpA on the nuclear translocation of NF-κB was studied (Fig. 5A). The optimum rGbpA concentration and incubation time for inducing NF-κB nuclear translocation were found to be 100 ng/well and 30 min, respectively, as determined by Western blotting with antibody against the p65 subunit of NF-κB. Levels of IκBα in the cytosolic fraction confirmed NF-κB translocation. Use of a proteasomal inhibitor (MG132) could almost block the nuclear translocation of NF-κB in rGbpA-stimulated HT-29 cells (Fig. 5B).

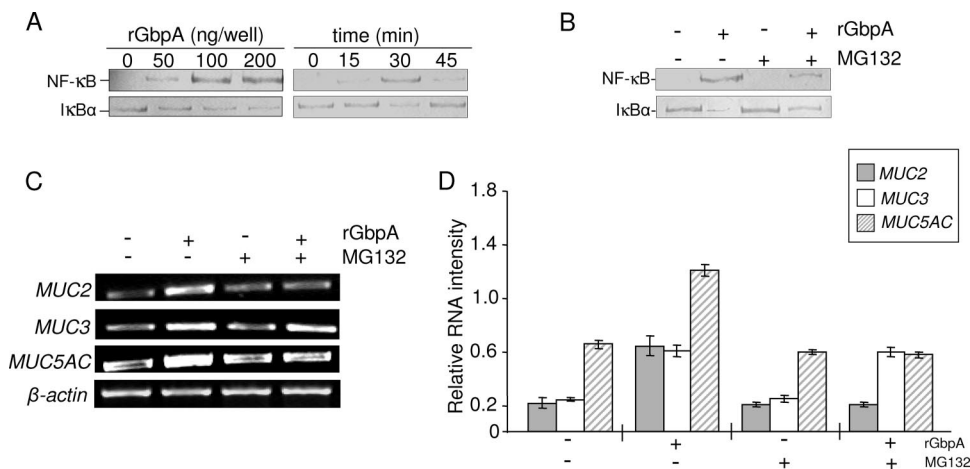Next, the effect of this inhibitor on mucin gene expression in

FIG. 5. Role of NF-κB in mucin gene upregulation. (A) rGbpA-induced nuclear translocation of NF-κB. Nuclear and cytosolic extracts were isolated from HT-29 cells treated with 0, 50, 100, or 200 ng/well rGbpA for 30 min. Similarly, extracts were prepared from the cells after treatment with 100 ng/well rGbpA for 0, 15, 30, or 45 min. Twenty micrograms of lysates was separated by SDS-PAGE, and Western blotting was performed with suitable antibodies as indicated. The blots shown here are representative of results obtained from three separate sets of experiments. (B) Inhibition of rGbpA-induced NF-κB nuclear translocation. HT-29 cells were treated with or without 100 ng/well rGbpA with or without pretreatment with MG132 (20 μM) for 30 min. Twenty micrograms of nuclear and cytosolic extracts were separated by SDS-PAGE, and Western blotting was performed with anti-NF-κB or anti-IκBα antibodies. The blots shown here are representative of results obtained from three separate sets of experiments. (C) Mucin gene upregulation by rGbpA involves NF-κB nuclear translocation. HT-29 cells were treated with or without 100 ng/well rGbpA with or without pretreatment for 30 min with 20 μM MG132. Total RNA was isolated, and RT-PCR was performed with primers specific for the MUC2, MUC3, MUC5AC, and β-actin genes. Equal amounts of RT-PCR products were run on 1% agarose gels. The β-actin gene was used as an internal control. A representative ethidium bromide-stained gel picture from three independent experiments is shown. (D) Normalized RT-PCR results are represented graphically. Equal amounts of RT-PCR products were run on 1% agarose gels, and gel images were analyzed densitometrically. PCR products were quantitated and expressed with respect to β-actin band intensity, which was taken as 1. Data represent means ± SEM from three independent experiments.

HT-29 cells was studied. The relative mRNA expression of MUC2, MUC3, and MUC5AC following incubation with or without rGbpA in presence or absence of MG132 was determined by RT-PCR (Fig. 5C and D). Pretreatment of cells with MG132 could prevent the upregulation of MUC2 and MUC5AC transcripts. MG132 had greater effects on regulation of MUC2 and MUC5AC transcript levels, suggesting that these genes require NF-κB activation during induction with GbpA.

Effect of intestinal mucus on GbpA expression in *V. cholerae*. Since GlcNAc could increase transcription of gbpA (7), we investigated the effect of different concentrations of mucin on gbpA expression. RT-PCR results revealed that intestinal mucin could increase expression of gbpA in N16961 (Fig. 6A and B). The increase of gbpA transcript in response to 0.5% to 2% intestinal mucin was within the linear range. The transcript increased 2.6-fold compared to the control ($P < 0.05$) when N16961 was grown in the presence of 2% mucin. No gbpA expression was observed in case of N1RB3 under these conditions (data not shown). In all cases, expression of internal control recA remained almost unchanged ($P = 0.251$).

Western blotting showed that mucin could indeed increase the level of GbpA in N16961 (Fig. 6C). As most of the GbpA is secreted, there was almost no detectable GbpA present on the bacterial surface before mucin exposure. However, a definite increase in the level of membrane-bound GbpA was observed after N16961 was grown in the presence of mucin. Confocal microscopy results showed that the level of GbpA on bacterial surface was very low prior to mucin exposure. This level increased when the bacteria were grown in the presence of mucin (Fig. 6D).

DISCUSSION

In order to understand the mechanism of intestinal adherence of *V. cholerae* and the exact role of GbpA in this process, we used a *V. cholerae* isogenic in-frame gbpA deletion mutant strain and an rGbpA protein. Confocal microscopy indicated that GbpA was responsible for the binding of the bacteria to the intestinal mucus layer quickly, at least initially, through a specific interaction. In vivo study with mouse model showed that without GbpA, *V. cholerae* could not colonize on mucus and failed to increase intestinal fluid secretion. This indicated that GbpA is initially involved in the intestinal adherence process. Since *V. cholerae* colonization is multifactorial (26), other adhesive factors are required for colonization, but not at the initial stage.

Binding studies with whole bacteria and mucin demonstrated that initially only a small number of wild-type bacteria could bind to mucin, but this interaction was dose dependent and saturable (R. Bhowmick et al., unpublished observation), indicating mucin as the intestinal receptor for GbpA. This could be explained by the fact that most of the GbpA is secreted and only a minor fraction remains on the outer surface of *V. cholerae* for adherence. Binding studies with rGbpA also showed concentration-dependent and saturable kinetics with mucin, with a K_d of 11.2 μM. This interaction could be specifically blocked with GlcNAc, indicating that rGbpA binds with GlcNAc residues of mucin. Interestingly, rGbpA showed similar K_ds with mouse IEC and their brush borders. The K_d for rGbpA was also found to be similar to those for other chitin-binding proteins (48). It is known from previous studies that,
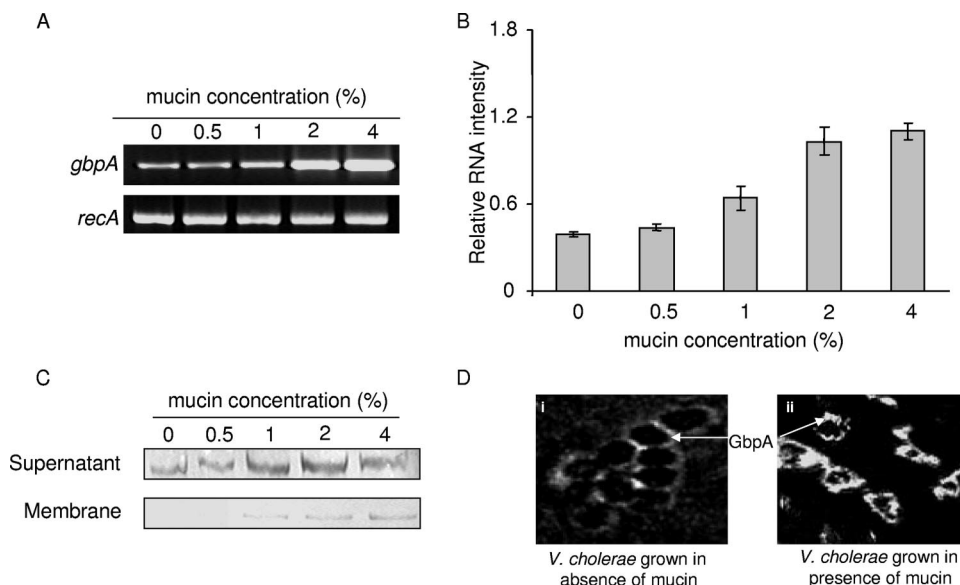
FIG. 6. Effect of intestinal mucus on GbpA expression. (A) RT-PCR analysis. N19691 was grown in the presence of 0 to 4% mouse intestinal mucin, keeping the other growth conditions the same. RT-PCR was performed using total RNA from mucin-treated or untreated N19691, using *gbpA* and *recA* gene-specific primers. Equal amounts of RT-PCR products were run on 1% agarose gels. *recA* was used as the internal control. A representative gel picture from three independent experiments is shown. (B) Normalized RT-PCR results are represented graphically. Ethidium bromide-stained PCR products were photographed, and the images were analyzed densitometrically. PCR products were quantitated and expressed with respect to *recA* band intensity, which was taken as 1. Data represent means ± SEM from three independent experiments. (C) N19691 was grown in the presence of 0 to 4% mouse intestinal mucin, keeping the other growth conditions the same. Membrane protein (20 μg) and culture supernatants (20 μg) were run on 10% SDS-PAGE, blotted, and probed with anti-rGbpA antibody. The blots shown here are representative of results obtained in three separate sets of experiments. (D) Surface localization of GbpA in N16961. Bacteria were grown in the absence (i) or presence (ii) of 2% mucin. The cells were harvested, and surface GbpA was probed with anti-rGbpA antibody and fluorescein isothiocyanate-labeled secondary antibody and observed at a magnification of ×100 under a confocal microscope. The bright white peripheries of cells indicate the GbpA localization. The confocal images presented here are representative of results obtained in three separate sets of experiments.

GlcNAc is present in the IEC surface (10), and results presented here indicate that GbpA binds only GlcNAc residues irrespective of the proteins on which they are present.

The GbpA-mediated binding of *V. cholerae* to mucin could increase mucus secretion in the intestine in a time-dependent manner, as evident from histopathology studies. Cholera toxin is also known to trigger mucin secretion in the small intestine (39); however, it is secreted only at a later stage (30). Previous studies have shown that this toxin does not lead to mucin secretion in HT-29 cells but can increase mucin secretion in intact mucosa, presumably through an indirect mechanism (31). Our results presented here show that rGbpA alone can stimulate mucus secretion in a time- and dose-dependent manner in HT-29 cells. Since only secreted mucins contribute to the formation of mucus gel of the intestine, we looked into MUC2, MUC3, and MUC5AC secretion (28, 39). We found that all three mucins showed increased secretion in the presence of rGbpA. We also found increases in their transcript levels, suggesting that rGbpA might increase mucus secretion transcriptionally.

Many bacterial products activate nuclear factor κB (NF-κB), which in turn plays a pivotal role in regulating many other genes (23). Here also, we found that NF-κB was activated and translocated into the nuclei of HT-29 cells in the presence of rGbpA. Thus, GbpA, being a bacterial component, was able initiate a signaling cascade leading to NF-κB activation in the intestinal cells. Previous reports have shown that mucin gene expression might increase under the influence of NF-κB (22). Here also, it can be presumed that NF-κB is involved as a downstream effector of the GbpA-induced signaling cascade resulting in increased mucus secretion. Pretreatment of HT-29 cells with the proteasomal inhibitor MG132 could significantly lower the rGbpA-induced nuclear translocation of NF-κB in HT-29 cells (24, 25), suggesting direct involvement of GbpA in NF-κB activation. Blocking of NF-κB translocation subsequently inhibited the upregulation of *MUC2* and *MUC5AC* transcripts, further establishing the role of NF-κB in the process. In case of *MUC3*, however, although rGbpA could induce its upregulation, transcript inhibition could not be observed within the time periods tested here. Since MUC2 and MUC5AC are the major components of secretory mucin (32), a role of NF-κB in GbpA-mediated mucin upregulation is clearly evident. However, further studies are required to understand the signal transduction cascade activated by GbpA through which GbpA enhances mucin secretion after binding to mucus.

On the other hand, we found that exposure to mucin significantly increased the level of GbpA in wild-type *V. cholerae* at both the RNA and protein levels. Again, this increase was dependent on concentration of mucin. It is possible that the induction of *gbpA* by mucin plays a significant role in increasing the number of GbpAs on the bacterial surface, which might overcome the initial constraint of less bacterial binding to

mucin, leading to better adherence and finally colonization on mucus.

Until now, it has remained elusive how a secretory protein could act as an adhesin, especially when GbpA could bind to mucin in a specific manner. Based on the results presented here, we propose how GbpA acts as the essential factor for the initial binding of *V. cholerae* to intestinal mucus. Initial binding of the bacteria occurs through interaction of GbpA with the GlcNAc residues of mucin. This increases intestinal mucus secretion through upregulation of mucin genes via NF-κB. As vibrios are chemotactically attracted to mucus (8), the increased mucin levels attract more bacteria to colonize the area and provide sufficient receptors for the formation of microcolonies. *V. cholerae* simultaneously uses this host response to increase the expression of GbpA. The increased levels of GbpA, especially on the bacterial surface, enhance efficient binding of the bacteria to the intestinal surface. From the results, it is clearly evident that GbpA and mucin increase each other in a time- and concentration-dependent manner. Thus, it can be said that this coordinated interaction between the host and the pathogen at the biochemical and functional levels lead to a vicious cycle of intestinal colonization by *V. cholerae* and ultimately initiate the disease. Our findings presented here are the first step toward understanding the mechanism of early adherence involving GbpA and highlight the possibility of inhibiting colonization by use of agents that block this interaction.

REFERENCES

1. **Akiba, Y., P. H. Guth, E. Engel, I. Nastaskin, and J. D. Kaunitz.** 2000. Dynamic regulation of mucus gel thickness in rat duodenum. Am. J. Physiol. Gastrointest. Liver Physiol. **279:**G437–G447.
2. **Alam, M., S. I. Miyoshi, K. I. Tomochika, and S. Shinoda.** 1997. *Vibrio mimicus* attaches to the intestinal mucosa by outer membrane hemagglutinins specific to polypeptide moieties of glycoproteins Infect. Immun. **65:** 3662–3665.
3. **Allen, A.** 1981. Structure and function of gastrointestinal mucus, p. 617–619. *In* L. R. Johnson (ed.), Physiology of the gastrointestinal tract. Raven Press, New York, NY.
4. **Angelichio, M. J., J. Spector, M. K. Waldor, and A. Camilli.** 1999. *Vibrio cholerae* intestinal population dynamics in the suckling mouse model of infection. Infect. Immun. **67:**3733–3739.
5. **Attridge, S. R., P. A. Manning, J. Holmgren, and G. Jonson.** 1996. Relative significance of mannose-sensitive haemagglutinin and toxin-coregulated pili in colonization of infant mice by *Vibrio cholerae* El Tor. Infect. Immun. **64:**3369–3373.
6. **Baselski, V., R. Briggs, and C. Parker.** 1977. Intestinal fluid accumulation induced by oral challenge with *Vibrio cholerae* or cholera toxin in infant mice. Infect. Immun. **15:**704–712.
7. **Bhowmick, R., A. Ghosal, and N. S. Chatterjee.** 2007. Effect of environmental factors on expression and activity of chitinase genes of vibrios with special reference to *Vibrio cholerae*. J. Appl. Microbiol. **103:**97–108.
8. **Bordas, M. A., M. C. Balebona, J. M. Rodriguez-Maroto, J. J. Borrego, and M. A. Morinigo.** 1998. Chemotaxis of pathogenic *Vibrio* strains towards mucus surfaces of gilthead sea bream (*Sparus aurata* L.). Appl. Environ. Microbiol. **64:**1573–1575.
9. **Cario, E., H. Goebell, and A. U. Dignass.** 1999. Factor XIII modulates intestinal epithelial wound healing in vitro. Scand. J. Gastroenterol. **34:**485–490.
10. **Chin, K., S. Onishi, M. Yuji, T. Inamoto, W. Qi, K. Yamamoto, K. Warita, T. Yokoyama, N. Hoshi, and H. Kitagawa.** 2007. Special sugar expression on apoptotic epithelial cells of Peyer's patches and intestinal villi in rat small intestine. J. Vet. Med. Sci. **69:**193–199.
11. **Chitnis, D. S., K. D. Sharma, and R. S. Kamat.** 1982. Role of somatic antigen of *Vibrio cholerae* in adhesion to intestinal mucosa. J. Med. Microbiol. **5:**53–61.
12. **Colwell, R. R., J. Kaper, and S. W. Joseph.** 1977. *Vibrio cholerae, Vibrio parahemolyticus,* and other vibrios: occurrence and distribution in Chesapeake Bay. Science **198:**394–396.
13. **Dean, E. A., and R. E. Isaacson.** 1982. In vitro adhesion of piliated *Escherichia coli* to small intestinal villous epithelial cells from rabbits and the identification of a soluble 987P pilus receptor-containing fraction. Infect. Immun. **36:**1192–1198.
14. **Dubois, M., K. A. Gilles, J. K. Hamilton, P. A. Rebers, and F. Smith.** 1956. Anal. Biochem. **28:**350.
15. **Fang, L., Z. Gan, and R. R. Marquardt.** 2000. Isolation, affinity purification, and identification of piglet small intestine mucosa receptor for enterotoxigenic *Escherichia coli* K88ac+ fimbriae. Infect. Immun. **68:**564–569.
16. **Florey, H.** 1955. Mucin and the protection of the body. Proc. R. Soc. London B **143:**144–158.
17. **Folders, J., J. Tommassen, L. C. Van Loon, and W. Bitter.** 2000. Identification of a chitin-binding protein secreted by *Pseudomonas aeruginosa.* J. Bacteriol. **182:**1257–1263.
18. **Gaudier, E., A. Jarry, H. M. Blottiere, P. de Coppet, M. P. Buisine, J. P. Aubert, C. Laboisse, C. Cherbut, and C. Hoebler.** 2004. Butyrate specifically modulates *MUC* gene expression in intestinal epithelial goblet cells deprived of glucose Am. J. Physiol. Gastrointest. Liver Physiol. **287:**G1168–G1174.
19. **Haller, D., M. P. Russo, R. B. Sartor, and C. Jobin.** 2002. IKKβ and phosphatidylinositol 3-kinase/Akt participate in non-pathogenic gram-negative enteric bacteria-induced RelA phosphorylation and NFκB activation in both primary and intestinal epithelial cell lines. J. Biol. Chem. **277:**38168–38178.
20. **Heidelberg, J. F., J. A. Eisen, W. C. Nelson, R. A. Clayton, M. L. Gwinn, R. J. Dodson, D. H. Haft, E. K. Hickey, J. D. Peterson, L. Umayam, S. R. Gill, K. E. Nelson, T. D. Read, H. Tettelin, D. Richardson, M. D. Ermolaeva, J. Vamathevan, S. Bass, H. Qin, I. Dragoi, P. Sellers, L. McDonald, T. Utterback, R. D. Fleishmann, W. C. Nierman, O. White, S. L. Salzberg, H. O. Smith, R. R. Colwell, J. J. Mekalanos, J. C. Venter, and C. M. Fraser.** 2000. DNA sequence of both chromosomes of the cholera pathogen *Vibrio cholerae*. Nature **406:**477–483.
21. **Henrissat, B.** 1991. A classification of glycosyl hydrolases based on amino acid sequence similarities. Biochem. J. **280:**309–316.
22. **Hybiske, K., J. K. Ichikawa, V. Huang, S. J. Lory, and T. E. Machen.** 2004. Cystic fibrosis airway epithelial cell polarity and bacterial flagellin determine host response to *Pseudomonas aeruginosa.* Cell. Microbiol. **6:**49–63.
23. **Ishida-Fujii, K., R. Sato, S. Goto, X. P. Yang, H. Kuboki, S. Hirano, and M. Sato.** 2007. Prevention of pathogenic *Escherichia coli* infection in mice and stimulation of macrophage activation in rats by an oral administration of probiotic *Lactobacillus casei* I-5. Biosci. Biotechnol. Biochem. **71:**866–873.
24. **Jobin, C., C. Hellerbrand, L. L. Licato, D. A. Brenner, and B. Sartor.** 1998. Mediation by NF-κB of cytokine induced expression of intercellular adhesion molecule 1 (ICAM-1) in an intestinal epithelial cell line, a process blocked by proteasome inhibitors. Gut **42:**779–787.
25. **Jono, H., T. Shuto, H. Xu, H. Kai, D. J. Lim, J. R. Gum, Y. S. Kim, S. Yamaoka, X. Feng, and J. Li.** 2002. Transforming growth factor-β-Smad signaling pathway cooperates with NFκB to mediate nontypeable *Haemophilus influenzae*-induced MUC2 mucin transcription. J. Biol. Chem. **277:** 45547–45557.
26. **Kaper, J. B., J. G. Morris, Jr., and M. M. Levine.** 1995. Cholera. Clin. Microbiol. Rev. **8:**48–86.
27. **Keyhani, N. O., and S. Roseman.** 1996. The chitin catabolic cascade in the marine bacterium *Vibrio furnissii.* Molecular cloning, isolation, and characterization of a periplasmic chitodextrinase. J. Biol. Chem. **271:**33414–33424.
28. **Khatri, I. A., C. Ho, R. D. Specian, and J. F. Forstner.** 2001. Characteristics of rodent intestinal mucin Muc3 and alterations in a mouse model of human cystic fibrosis. Am. J. Physiol. Gastrointest. Liver Physiol. **280:**G1321–G1330.
29. **Kirn, T. J., B. A. Jude, and R. K. Taylor.** 2005. A colonization factor links *V. cholerae* environmental survival and human infection. Nature **438:**863–866.
30. **Lee, S. H., D. L. Hava, M. K. Waldor, and A. Camilli.** 1999. Regulation and temporal expression patterns of *Vibrio cholerae* virulence genes during infection. Cell **99:**625–634.
31. **Lencer, W. I., F. D. Reinhart, and M. R. Neutra.** 1990. Interaction of cholera toxin with cloned human goblet cells in monolayer culture. Am. J. Physiol. **258:**G96–G102.
32. **Liévin-Le Moal, V., G. Huet, J. P. Aubert, J. Bara, M. E. Forgue-Lafitte, A. L. Servin, and M. H. Coconnier.** 2002. Activation of mucin exocytosis and upregulation of *MUC* genes in polarized human intestinal mucin-secreting cells by the thiol-activated exotoxin listeriolysin O. Cell. Microbiol. **8:**515–529.
33. **Lipp, E. K., A. Huq, and R. R. Colwell.** 2002. Effects of global climate on infectious disease: the cholera model. Clin. Microbiol. Rev. **15:**757–770.
34. **Lowry, O. H., N. J. Rosebrough, A. L. Farr, and R. J. Randall.** 1951. Protein measurement with the Folin phenol reagent. J. Biol. Chem. **193:**265–275.

35. **Mantle, M., and A. Allen.** 1978. Colorimetric assay for glycoproteins based on the periodic acid/Schiff stain. Biochem. Soc. Trans. **6:**607–609.

36. **Mantle, M., and A. Allen.** 1981. Isolation and characterization of native glycoprotein from pig small-intestinal mucus. Biochem. J. **195:**267–275.

37. **Meibom, K. L., X. B. Li, A. T. Nielsen, C. Wu, S. Roseman, and G. K. Schoolnik.** 2004. The *Vibrio cholerae* chitin utilization program. Proc. Natl. Acad. Sci. USA **101:**2524–2529.

38. **Miller, V. L., and J. J. Mekalanos.** 1988. A novel suicide vector and its use in construction of insertion mutations: osmoregulation of outer membrane proteins and virulence determinants in *Vibrio cholerae* requires ToxR. J. Bacteriol. **170:**2575–2583.

39. **Moncada, D. M., S. J. Kammanadiminti, and K. Chadee.** 2003. Mucin and Toll-like receptors in host defense against intestinal parasites. Trends Parasitol. **19:**305–311.

40. **Montgomery, M. T., and D. L. Kirchman.** 1993. Role of chitin-binding proteins in the specific attachment of the marine bacterium *Vibrio harveyi* to chitin. Appl. Environ. Microbiol. **59:**373–379.

41. **Neutra, M. R., and J. F. Forstner.** 1987. Gastrointestinal mucus: synthesis, secretion and function, p. 975–1009. *In* L. R. Johnson (ed.), Physiology of the gastrointestinal tract. Raven Press, New York, NY.

42. **Reidl, J., and K. E. Klose.** 2002. *Vibrio cholerae* and cholera: out of the water and into the host. FEMS Microbiol. Rev. **26:**125–139.

43. **Saha, N., and K. K. Banerjee.** 1995. Carbohydrate-dependent binding of the cell-free hemagglutinin of *Vibrio cholerae* to glycoprotein and glycolipid. J. Bacteriol. **177:**758–764.

44. **Sambrook, J., and D. W. Russell.** 2001. Molecular cloning: a laboratory manual, 3rd ed. Cold Spring Harbor Laboratory, Cold Spring Harbor, NY.

45. **Schreiber, E., P. Matthias, M. M. Muller, and W. Schaffner.** 1989. Rapid detection of octamer binding proteins with 'mini-extracts,' prepared from a small number of cells. Nucleic Acids Res. **17:**6419.

46. **Skorupski, K., and R. K. Taylor.** 1996. Positive selection of vectors for allelic exchange. Gene **169:**47–52.

47. **Taylor, R. K., V. L. Miller, D. B. Furlong, and J. J. Mekalanos.** 1987. Use of phoA gene fusions to identify a pilus colonization factor coordinately regulated with cholera toxin. Proc. Natl. Acad. Sci. USA **84:**2833–2837.

48. **Vaaje-Kolstad, G., D. R. Houston, A. H. K. Riemen, V. G. H. Eijsink, and D. M. F. van Aalten.** 2005. Crystal structure and binding properties of the *Serratia marcescens* chitin-binding protein CBP21. J. Biol. Chem. **280:**11313–11319.

49. **Vesterlund, S., J. Paltta, M. Karp, and A. C. Ouwehand.** 2005. Adhesion of bacteria to resected human colonic tissue: quantitative analysis of bacterial adhesion and viability. Res. Microbiol. **156:**238–244.

50. **Watnick, P. I., K. J. Fullner, and R. Kolter.** 1999. A role for the mannose-sensitive hemagglutinin in biofilm formation by *Vibrio cholerae* El Tor. J. Bacteriol. **181:**3606–3609.

51. **Yamamoto, T., T. Kamano, M. Uchimura, M. Iwanaga, and T. Yokota.** 1988. *Vibrio cholerae* O1 adherence to villi and lymphoid follicle epithelium: in vitro model using formalin-treated human small intestine and correlation between adherence and cell associated hemagglutinin levels. Infect. Immun. **56:**3241–3250.

52. **Yamamoto, T., and T. Yokota.** 1988. Electron microscopic study of *Vibrio cholerae* O1 adherence to the mucus coat and villus surface in the human small intestine. Infect. Immun. **56:**2753–2759.